J. Phys. Chem. A **2005,** *109,* 11975−11979 **11975**

Theoretical Study of the Stability of Lithium Atoms in α-Rhombohedral Boron

Wataru Hayami,* Takaho Tanaka, and Shigeki Otani

Advanced Materials Laboratory, National Institute for Materials Science, 1-1 Namiki, Tsukuba, Ibaraki 305-0044, Japan

Received: June 7, 2005; In Final Form: October 6, 2005

The stability of lithium atoms in α-rhombohedral boron was investigated by first-principles calculations of total energies and molecular dynamics (MD) simulations. In the case of a low concentration (1.03 at. %), Li at the center of the icosahedral B_{12} site (the I-site) had a negative binding energy, which suggests Li at the I-site is unstable. However, MD simulations at temperatures below 750 K indicated that Li is still confined in the B_{12} cage under these conditions, which means Li at the I-site is metastable. Over 800 K, Li began to move away from the B_{12} site and settled at the tetrahedral site (the T-site) or at the octahedral site (the O-site). Li at the T-site also had a negative binding energy, but MD simulations indicated it was metastable up to 1400 K and did not move to other sites. Li at the O-site was energetically the most favorable, having a positive binding energy. In the case of a high concentration (7.69 at. %), the I-site changed to an unstable saddle point. At this concentration, the T-site was metastable and the O-site became the most stable. In MD simulations at 1400 K, Li atoms at the O-site never jumped to other sites regardless of concentration. Considering these facts, the diffusion coefficient of Li in α-rhombohedral boron would have to be very small below 1400 K.

Introduction

Boron forms compounds with a variety of structures due to its covalency.[1] The arrangement of boron atoms in these compounds depends on the composition ratio. In binary compounds (MB, M_3B_4, M = metal atom), boron atoms tend to form linear chains. As the amount of boron in a material increases, the boron atoms form a two-dimensional network (MB_2, M_2B_5) and eventually a three-dimensional framework (MB_4, MB_6, MB_{12}, MB_{66}, etc.). The multiformity of these structures has some similarities to those of carbon, but boron-based structures have a characteristic icosahedral structure comprised of 12 atoms, which is ubiquitously found in elemental boron and boron-rich compounds. Icosahedoral structures with 13 atoms are often observed in metallic clusters because 13 atoms can favorably form a close-packed structure. However, in the case of B_{12}, there is a vacancy at the center. This unique structure and, as a result, unique properties have attracted a great deal of attention in the form of both experimental and theoretical studies.

α-Rhombohedral (α-rh) boron is the simplest polymorph of elemental boron (Figure 1), having one B_{12} icosahedron/unit cell. This structure was first determined by Decker and Kasper[2] and later refined by Morosin et al.[3] and Will et al.[4] Theoretical studies on α-rh boron and related compounds such as $B_{12}P_2$, $B_{12}As_2$, $B_{12}O_2$, and $B_{12}C_3$ have been reported.[7−25] Intercalated atoms, P, As, and O, are on the diagonal axis around the center of the unit cell.[3,5,6] Theoretical studies of B_{12} and other boron clusters have also been conducted.[26−33] Intercalation into the center of a B_{12} icosahedron has yet to be observed in any boron compound. This suggests that it is difficult to thermally dope an atom into the icosahedron. However, as in the case of fullerene, a reaction promoted by a larger source of energy (arc discharge, ion implantation, etc.) might make this doping possible, assuming the doped structure is stable or metastable. If this doping can be achieved, numerous new materials with $X@B_{12}$ (an X atom in a B_{12} icosahedron) structural units will be possible. For this reason, it is important to study the stabilities of B_{12} and $X@B_{12}$ icosahedra in order to find potential dopants.

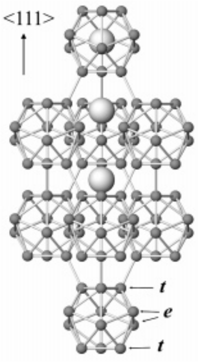

Figure 1. Structure of α-rhombohedral boron. Boron atoms (small spheres) form icosahedra, and the icosahedra form a rhombohedral lattice. Large spheres indicate three possible Li sites, icosahedral (I), tetrahedral (T), and octahedral (O), from top to bottom. The B atoms in an icosahedron are classified into two groups, six B atoms, denoted by "*t*", that make bonds with neighboring icosahedra and the other six B atoms, denoted by "*e*".

A theoretical study by Kawai[26] showed that the B_{13} icosahedron is not stable. Another first-principles calculation by Gunji[14] showed that $Li@B_{12}$ (a Li atom in the B_{12} cage) is energetically unstable with α-rhombohedral (α-rh) boron but that $Li@Li_3B_{12}$ (a Li atom in the B_{12} cage and three Li atoms in the intercalation sites) is stable. In theoretical work by Hayami,[30] calculations using cluster models AB_{12} (A = H−Ne) suggested that H and Li atoms could occupy the B_{12} cage. Experimentally, Soga et al.[34] and Terauchi et al.[35] produced a Li- and Mg-doped α and *β*-rhombohedral (*β*-rh) boron and examined its atomic and electronic properties. In the case of

---

* Corresponding author. E-mail: hayami.wataru@nims.go.jp.

10.1021/jp053031v CCC: $30.25

the Li-doped α-rh boron, they observed a slight increase in the density of states at the Fermi level by electron energy loss spectroscopy (EELS). Comparing the EELS spectra and the calculated density of states in previous work,[14] the number of Li atoms was found to be small, indicating Li was probably not in the B_{12} cage but rather in the intercalation sites. The precise location of Li was unknown since the X-ray diffraction pattern exhibited little change with the Li doping. In the former calculations,[14,30] the concentration of Li to boron was rather large, at least one Li to each B_{12} icosahedron, and it is not known if $Li@B_{12}$ is stable or not at low Li concentrations, which would likely represent the practical cases.

We chose Li among the possible dopants because it is a promising candidate according to our previous study,[30] and the experimental data to compare are available.[34,35] First-principles calculations using a large unit cell ($B_{96} = (B_{12})_8$) with Li as the dopant were performed to investigate the stability of $Li@B_{12}$. The total energies of the optimized structures were calculated, followed by molecular dynamics (MD) simulations at finite temperatures. The stabilities of Li at the other sites were also investigated to compare with the experimental data.

Computational Method

The calculation of the total energies and the Car−Parrinello molecular dynamics[36] were performed using the CPMD code version 3.9.1.[37,38] This code is based on the density functional theory[39,40] with plane waves and pseudopotentials. The norm-conserving, Troullier−Martins type pseudopotentials[41] were used. The generalized gradient approximation was included with the functional derived by Becke[42] and Lee−Yang−Parr.[43] An energy cutoff of 40 Ry was enough to provide a convergence of the total energy. Since the unit cell is large, *k*-point sampling in the total energy calculation was done using Monkhorst−Pack sampling[44] of a $(2 \times 2 \times 2)$ mesh. The results were compared with those of a finer mesh, and it was found that the difference in the total energy per atom was less than 6×10^{-4} eV. For the MD, the calculations were performed only at the Γ point. The temperature was controlled by scaling the total kinetic energy of the atoms at every time step. The time step was 5.0 a.u. (0.121 fs). The jobs were executed in parallel on a cluster computer equipped with eight CPUs. The CPU time for one step in the MD simulation with B_{96} atoms was about 4 s.

Results and Discussion

Figure 1 depicts the structure of α-rh boron. A unit cell consists of a B_{12} icosahedron stacked as in an fcc structure along the ⟨111⟩ direction. Experimental data for the lattice parameters are $a = 5.0643$ Å and $\alpha = 58.0962°$. ($\alpha = 60°$ in an ideal fcc structure.[3]) In our model, a $2 \times 2 \times 2$ unit cell comprised of $(B_{12})_8 = B_{96}$ atoms was used. The large spheres in the figure indicate three possible Li sites, icosahedral (I), tetrahedral (T), and octahedral (O) from top to bottom. The T-site is the center of four B_{12} clusters, and the O-site is the center of the ⟨111⟩ diagonal axis of the unit cell. The calculated lattice parameters, $a = 5.04$ Å and $\alpha = 58.6°$, were close to the experimental values. The calculated cohesive energy per boron atom, 5.93 eV/atom, was also close to the experimental value, 5.81 eV/atom.[45] These results guarantee the accuracy of calculations.

First, one Li atom was placed on the I-site and the structure was optimized. The concentration of Li was about 1.03 at. %, which is much smaller than in previous studies.[14,30] When the geometry was fully optimized, Li still remained at the I-site. However, the binding energy, defined here as $E(B_{96}) + E(\text{Li}) - E(\text{LiB}_{96})$, where E is the total energy, was −4.99 eV. A negative binding energy indicates that the I-site for Li is not globally stable but instead is metastable, or a saddle point. To obtain more information about the stability of Li at this location, Car−Parrinello MD simulations were performed at various temperatures. Figure 2 shows the trajectories of Li and the surrounding B atoms projected onto a plane normal to the ⟨111⟩ direction. Only six *e*-borons (see Figure 1) are plotted. At 300 K, the Li atom oscillates around the center of the icosahedron while the icosahedron keeps its structure. Therefore, the I-site for Li is not a saddle point but a metastable site. At a temperature around 700−750 K, the icosahedron begins to deform. In Figure 2b,c, the bottom and the right bottom B are moving separately, and at 800 K, Li finally escapes from the B_{12} cage. The escape temperature is estimated to be 775 ± 25 K, corresponding to a potential barrier of 67 ± 2.2 meV. This value is much smaller than the absolute value of the binding energy. After moving out of the cage, Li settled at the O-site at 800 K, but it settled at the T-site in a simulation at 1200 K. The potential barrier to the O-site may be a little lower than that to the I-site, but a lot more MD simulations are required to make a statistically meaningful estimation.

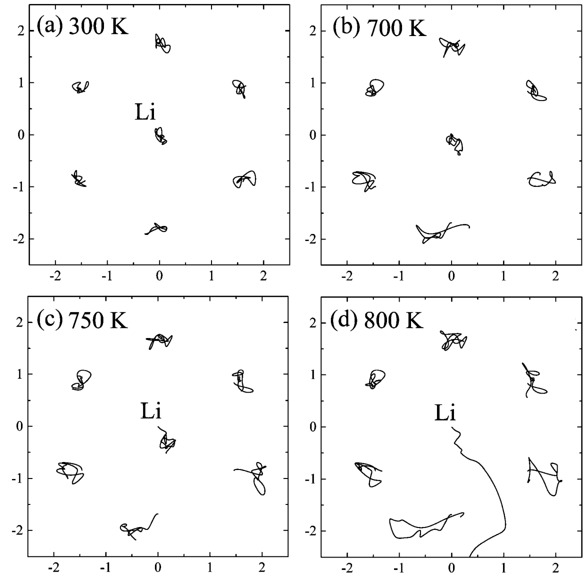

Figure 2. Trajectories of Li atoms at the I-site and the surrounding six *e*-B atoms. The projection plane is normal to the ⟨111⟩ direction. The unit of scale is angstroms. The time step is 0.121 fs, and the number of steps is 2000 (241.8 fs). Key: (a): $T = 300$ K; (b) $T = 700$ K; (c) $T = 750$ K; (d) $T = 800$ K. At 800 K, Li escapes out of the B_{12} cage.

Next, an Li atom was placed at the T- and at the O-site and the total energies were calculated after optimizing the geometries. In both cases, Li stayed at each site. The binding energies for Li are −1.04 eV (T-site) and +0.17 eV (O-site). Therefore, only the O-site is energetically stable. These results cannot be compared directly with the results by Gunji et al.[14] because of differences in the Li concentration, but both results exhibited a similar tendency in that the O-site was the most stable and the I-site produced a negative binding energy for Li. As in the case of the I-site, MD simulations were performed for both the T- and the O-sites.

Figure 3 shows the projected trajectories at 1400 K. Parts a and c are on the planes normal to the ⟨111⟩ direction, and parts b and d are parallel to the ⟨111⟩ direction. At the T-site (Figure 3a,b), Li moves in a relatively localized area, with the distribution of the trajectory being almost isotropic. At the O-site, the Li trajectory was spread over a wider area on the plane normal to the ⟨111⟩ direction (Figure 3c) but not to the ⟨111⟩ direction (Figure 3d). This suggests that the potential

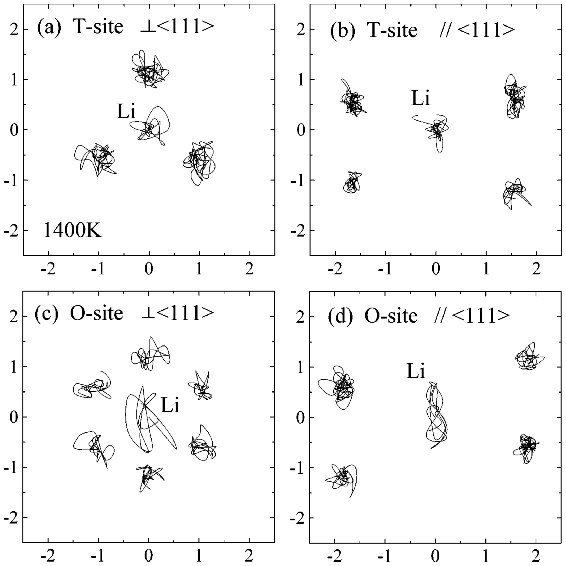

Figure 3. Trajectories of Li at the T-site and the O-site. The temperature is 1400 K. The unit of scale is angstroms. The time step is 0.121 fs, and the number of steps is 4000 (483.8 fs). The projection plane is normal to the ⟨111⟩ direction for (a) and (c) and parallel for (b) and (d). (a, b): Li atom at the T-site and six neighboring B atoms. (c, d): Li atom at the O-site and six neighboring B atoms.

TABLE 1: Binding Energies, Potential Barriers, and Li−B Distances for LiB_{96}[a]

site	binding energy (eV)	potential barrier (eV)	Li−B dist (Å)
I-site	−4.99	0.067 (775 K)	1.76
T-site	−1.04	>0.12 (1400 K)	1.91
O-site	0.17	stable	2.18

[a] Only the O-site is energetically stable, while the other two sites are metastable. The potential barrier between the T- and O-sites is not exactly known (more than 1400 K = 0.12 eV).

barrier is steeper in the ⟨111⟩ direction. For both the T- and O-sites, Li does not migrate out of the sites at this temperature. This indicates that the T-site is metastable and the O-site is stable. The binding energies for Li are summarized in Table 1. The potential barrier between the T- and O-sites is not exactly known (over 1400 K). An MD simulation at higher temperatures is meaningless for the present purposes because the phase transition to β-rh boron occurs at 1400 K.[46] For compounds such as boron phosphide $B_{12}P_2$, P is located between the T- and O-sites,[3,5,6] but no metastable points for a single Li were observed at these locations in this study.

With respect to the binding energy, only the O-site has a positive value such that Li could be thermally doped into this site. However, considering the potential barrier to neighboring sites, it is likely that the diffusion coefficient of Li is very small below 1400 K. This explains why Li was doped only in a small part of the sample,[34,35] and the amount of Li is small even in the doped areas. Thermal doping may proceed through defects or grain boundaries.

The bond lengths of α-rh boron with a Li atom at the I-site are listed in Table 2. The calculated bond lengths of pure boron (a) are in good agreement with the experimental values (d).[3,4] The calculated error is less than 1.2% for intraicosahedron (intra) bonds and the *t*−*t* bonds in the intericosahedron (inter). For the inter *e*−*e* bonds, the error is a little larger (2.2%). It is well-known that the inter *t*−*t* bond is shorter than the intra *t*−*t* bond. When a Li atom is put at one of the I-sites, the total icosahedron deforms (b). The regular triangle composed of intra *t*−*t*−*t* bonds transforms to an isosceles triangle. The intra *t*−*t* bond expands by 2.3−4.6%, the intra *t*−*e* bond by 2.8−7.9%, and the intra *e*−*e* bond by 3.4−6.8%. The expansion rate for *t*−*t* is a little smaller than the other two, which would reflect the strength of these bonds. Interestingly, Li always leaves the B_{12} cage through the *e*-borons. On the other hand, the inter *t*−*t* and *e*−*e* bonds contract by 2.4% and 2.9−4.9%, respectively. Since the expansion of the icosahedron is made possible by these interbond contractions, additional Li atoms at the I-sites may weaken the icosahedra. The bond lengths of B_{12} without Li do not change as much (c).

To observe the stability of Li at a high concentration, eight Li atoms were put on the I-, T-, and O-sites in the 2 × 2 × 2 cell (Li_8B_{96} = $(LiB_{12})_8$). The concentration of Li was 7.69 at. %. The binding energies per Li atom and the optimized cell parameters are listed in Table 3. Here, the binding energy is defined as $\{E(B_{96}) + 8E(Li) - E(Li_8B_{96})\}/8$. For all of the sites, the binding energies were only slightly higher (more stable) than in the case of LiB_{96} (Table 1), and the energy differences between the sites were similar. In a previous report,[14] the difference between the I-site (−2.86 eV) and the O-site (2.38 eV) was listed as 5.24 eV, which is close to the result in this study (5.01 eV), but the absolute binding energies are about 2 eV higher in our results. This discrepancy can probably be attributed to the difference in the method of geometrical optimization, basis functions, and the exchange-correlation functional. Compared with the calculated values without Li, the lattice parameters expanded by 3.2% for the I- and T-sites and by 2.0% for the O-site. The changes in the interaxis angle α were generally small.

MD simulations at finite temperatures were performed to check the stability of Li_8B_{96}. At 800 K, Li atoms at I-sites immediately moved out of B_{12} cages, so that we lowered temperature in order to find if Li atoms could remain at the I-sites at any temperature. Figure 4 shows snapshots of an MD simulation at 10 K. At first, the Li atom remains at the center for a moment (Figure 4a). Once the Li atom shifts from the center, it quickly slips out of the cage (Figure 4b−d). This means that the I-site is almost unstable (probably a saddle point). When the Li atom is moving out of the cage, it always breaks the

TABLE 2: Bond Lengths of α-Rh Boron with a Li Atom at the I-Site

	intraicosahedron (Å)			intericosahedron (Å)	
	t−*t*	*t*−*e*	*e*−*e*	*t*−*t*	*e*−*e*
$(B_{12})_8$[a]	1.75	1.78	1.77	1.68	2.06
Li$(B_{12})_8$ (I-site) B_{12} including Li[b]	1.79−1.83 (2.3−4.6%)	1.83−1.92 (2.8−7.9%)	1.83−1.89 (3.4−6.8%)	1.64 (−2.4%)	1.96−2.00 (−4.9 to −2.9%)
Li$(B_{12})_8$ (I-site) B_{12} without Li[c]	1.75	1.769−1.799	1.75−1.77	1.67−1.68	2.044−2.117
expt[d]	1.754	1.80	1.784	1.671	2.013

[a] Pure boron (calculated). [b] B_{12} icosahedron including Li. The numbers in parentheses are the expansion rates compared with the case for footnote *a*. [c] B_{12} icosahedron without Li. [d] The experimental values taken from refs 3 and 4.

TABLE 3: Binding Energies per Li Atom, Potential Barriers, Optimized Lattice Parameters, and Li−B Distances of Li_8B_{96}[a]

	binding energy (eV)	potential barrier (eV)	lattice param		
			a (Å)	α (deg)	Li−B dist (Å)
I-site	−4.60	∼0	5.20	58.1	1.79
T-site	−0.71	0.08 (925 K)	5.20	58.4	1.93
O-site	0.41	stable	5.14	57.7	2.23

[a] All three sites have a slightly higher binding energy than in the LiB_{96} case. The I-site becomes unstable, and the potential barrier for the T-site is lowered (see text).

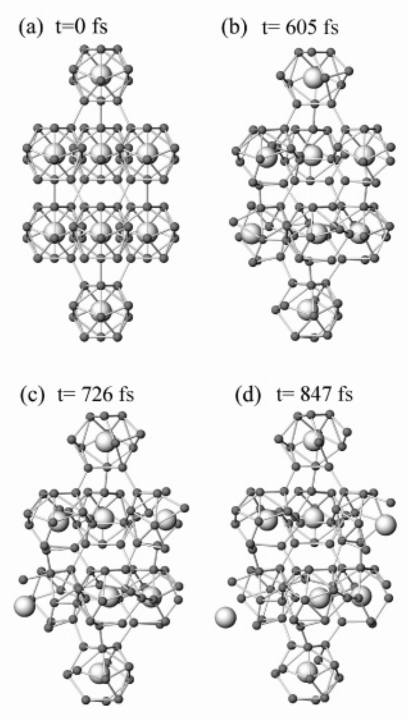

Figure 4. MD simulations of Li at the I-site at 10 K: (a) $t = 0$; (b) $t = 605$ fs (Li atom at the bottom-left begins to move); (c) $t = 726$ fs (another Li at the top-right begins to move); (d) $t = 847$ fs (bottom-left Li moves toward the O-site).

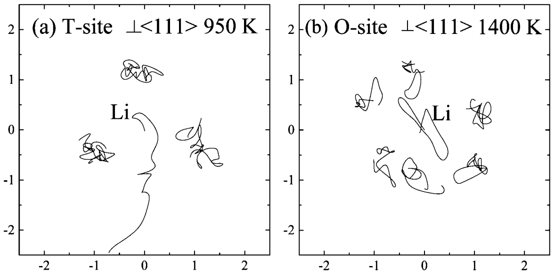

Figure 5. Trajectories of Li (a) at the T-site at 950 K and (b) at the O-site at 1400 K. The unit of scale is angstroms. The time step is 0.121 fs, and the number of steps is 2000 (241.9 fs). The projection plane is normal to the ⟨111⟩ direction.

intra $e-e$ bonds, which would suggest that the intra $e-e$ bonds are weaker than the intra $t-t$ bonds.

MD simulations with eight Li atoms at the T-site indicated that Li atoms begin to hop to the O-site at about 950 K (Figure 5a). The T-site is metastable but not as stable as in the low concentration case, in which Li hopping did not occur below 1400 K (Figure 3). Simulations with eight Li atoms at the O-site indicated that the O-site is stable up to 1400 K (Figure 5b). Considering these results, the most stable site for Li is the O-site regardless of Li concentration. It is also clear the thermal diffusion of Li in α-rh boron is obstructed by the high potential barrier.

Conclusions

The stability of Li in α-rh boron was investigated by first-principles calculations of the total energies and molecular dynamics simulations. At low concentrations (LiB_{96}), Li at the I-site is metastable up to 775 ± 25 K, metastable at the T-site up to 1400 K, and is most stable at the O-site. Only the O-site has a positive binding energy. At high concentrations ($(LiB_{12})_8$), the I-site becomes less stable (saddle point) and the T-site remains metastable up to 925 ± 25 K. In every case, the O-site is the most stable. Independent of the concentration, Li at the O-site does not migrate to the other sites below 1400 K, indicating a small diffusion coefficient, which is in agreement with past experimental results.

Since Li at the I-site was proven to be metastable at low concentrations, the $Li@B_{12}$ structure could theoretically form. However, since the total energy of Li at the I-site is much higher (5.01−5.16 eV) than that at the O-site and the stabilizing energy is very small (0.067 eV = 775 K), it would not be easy to attain this structure experimentally. That may possibly be achieved by a method like the ion implantation with precisely controlled energy.

Acknowledgment. We thank Takashi Aizawa for valuable discussions.

References and Notes

(1) Adams, R. M. *Boron, Metallo-Boron Compounds and Boranes*; Interscience Publishers: John Wiley & Sons: New York, 1964.
(2) Decker, B. F.; Kasper, J. S. *Acta Crystallogr.* **1959**, *12*, 503.
(3) Morosin, B.; Mullendore, A. W.; Emin, D.; Slack, G. A. *AIP Conference Proceedings 140*; Am. Inst. Phys: New York, 1986; p 70.
(4) Will, G.; Kiefer, B. *Z. Anorg. Allg. Chem.* **2001**, *627*, 2100.
(5) Slack, G. A.; McNelly, T. F.; Taft, E. A. *J. Phys. Chem. Solids* **1983**, *44*, 1009.
(6) Yang, P.; Aselage, T. L. *Powder Diffr.* **1995**, *10*, 263.
(7) Longuet-Higgins, H. C.; Roberts, M. deV. *Proc. R. Soc. London* **1955**, *230A*, 110.
(8) Bullett, D. W. *J. Phys C: Solid State Phys.* **1982**, *15*, 415.
(9) Lee, S.; Bylander, D. M.; Kleinman, L. *Phys. Rev. B* **1990**, *42*, 1316.
(10) Bylander, D. M.; Kleinman, L.; Lee, S. *Phys. Rev. B* **1990**, *42*, 1394.
(11) Beckel, C. L.; Yousaf, M.; Fuka, M. Z.; Raja, S. Y.; Lu, N. *Phys. Rev. B* **1991**, *44*, 2535.
(12) Lee, S.; Bylander, D. M.; Kleinman, L. *Phys. Rev. B* **1992**, *45*, 3245.
(13) Gunji, S.; Kamimura, H.; Nakayama, T. *J. Phys. Soc. Jpn.* **1993**, *62*, 2408.
(14) Gunji, S.; Kamimura, H. *Phys. Rev. B* **1996**, *54*, 13665.
(15) Li, D.; Ching, W. Y. *Phys. Rev. B* **1995**, *52*, 17073.
(16) Vast, N.; Baroni, S.; Zerah, G.; Besson, J. M.; Polian, A.; Grimsditch, M.; Chervin, J. C. *Phys. Rev. Lett.* **1997**, *78*, 693.
(17) Vast, N.; M. Besson, J.; Baroni, S.; Dal Corso, A. *Comput. Mater. Sci.* **2000**, *17*, 127.
(18) Shirai, K.; Katayama-Yoshida, H. *J. Phys. Soc. Jpn.* **1998**, *67*, 3801; *Physica B* **1999**, *263−264*, 791.
(19) Fujimori, M.; Nakata, T.; Nakayama, T.; Nishibori, E.; Kimura, K.; Takata, M.; Sakata, M. *Phys. Rev. Lett.* **1999**, *82*, 4452.
(20) Zhao, J.; Lu, J. P. *Phys. Rev. B* **2002**, *66*, 092101.
(21) Masago, A.; Shirai, K.; Katayama-Yoshida, H. *Mol. Simul.* **2004**, *30*, 935.
(22) Shirai, K.; Masago, A.; Katayama-Yoshida, H. *Phys. Status Solidi b* **2004**, *241*, 3161.
(23) Emin, D.; Evans, D. G.; McCready, S. S. *Phys. Status Solidi b* **1998**, *205*, 311.
(24) Emin, D. *Solid. State Chem.* **2004**, *177*, 1619; *Phys. Rev. B* **2000**, *61*, 6069; *Phys. Rev. B* **1999**, *59*, 6205.
(25) Aselage, T. L.; Emin, D.; McCready, S. S. *Phys. Rev. B* **2001**, *64*, 054302; *Phys. Status Solidi b* **2000**, *218*, 255.
(26) Kawai, R.; Weare, J. H. *Chem. Phys. Lett.* **1992**, *191*, 311.

(27) Kato, H.; Yamashita, K.; Morokuma, K. Bull. *Chem. Soc. Jpn*. **1993**, *66*, 3358.

(28) Fujimori, M.; Kimura, K. *J. Solid. State. Chem.* **1997**, *133*, 178.

(29) Gu, F.; Yang, X.; Tang, A.; Jiao, H.; Schleyer, P. *J. Comput. Chem.* **1998**, *19*, 203.

(30) Hayami, W. *Phys. Rev. B* **1999**, *60*, 1523.

(31) Boustani, I. *Chem. Phys. Lett.* **1995**, *240*, 135; *Phys. Rev. B* **1997**, *55*, 16426; *J. Solid State Chem.* **1997**, *133*, 182.

(32) Chacko, S.; Kanhere, D. G.; Boustani, I. *Phys. Rev. B* **2003**, *68*, 035414.

(33) Xu, S. J.; Nilles, J. M.; Radisic, D.; Zheng, W. J.; Stokes, S.; Bowen, K. H.; Becker, R. C.; Boustani, I. *Chem. Phys. Lett* **2003**, *379*, 282.

(34) Soga, K.; Oguri, A.; Araake, S.; Terauchi, M.; Fujiwara, A.; Kimura, K. *J. Solid State Chem.* **2004**, *177*, 498.

(35) Terauchi, M.; Oguri, A.; Kimura, K.; Fujiwara, A. *J. Electron Microsc.* **2004**, *53*, 589.

(36) Car, R.; Parrinello, M. *Phys. Rev. Lett.* **1985**, *55*, 2471.

(37) *CPMD*; IBM Corp., Armonk, NY, 1990−2004, MPI fur Festkorperforschung, Stuttgart, Germany, 1997−2001; http://www.cpmd.org/.

(38) Marx, D.; Hutter, J. *NIC Series*; John von Neumann Institute for Computing: Jülich, Germany, 2000; Vol. 1, pp 301−449.

(39) Hohenberg, P.; Kohn, W. *Phys. Rev.* **1964**, *136*, B864.

(40) Kohn, W.; Sham, L. J. *Phys. Rev.* **1965**, *140*, A1133.

(41) Troullier, N.; Martins, J. L. *Phys. Rev. B* **1991**, *43*, 1993.

(42) Becke, A. D. *Phys. Rev. A* **1988**, *38*, 3098.

(43) Lee, C.; Yang, W.; Parr, R. G. *Phys. Rev. B* **1988**, *37*, 785.

(44) Monkhorst, H. J.; Pack, J. D. *Phys. Rev. B.* **1976**, *13*, 5188.

(45) Kittel, C. *Introduction to Solid State Physics*, 6th ed.; Wiley: New York, 1986; p 55.

(46) Runow, P. *J. Mater. Sci.* **1972**, *7*, 499.